

Electrochemical studies of methyl-3-benzoyl indolizine carboxylates

Eleonora-Mihaela UNGUREANU^{*a}, Maria-Laura SOARE^a, Herve HUSER^b and Emilian GEORGESCU^c.

^a Faculty of Applied Chemistry and Material Sciences, University "Politehnica" of Bucharest, Splaiul Independentei, 313, 060042, Bucharest, Romania

^b Faculté des Sciences Fondamentales et Appliquées- Chimie, 40 av. du recteur Pineau, 86022 Poitiers, France

^c S.C. Oltchim S.A., Uzinei Street, 1, 240050, Ramnicu Valcea, Romania

Abstract Indolizine derivatives have been used in medicine and pharmacology due to their biological activity and therapeutical effects. Their capacity to form surface films and to be used as sensors in modern technologies makes them interesting to be studied.

This work is devoted to the study of methyl-3-benzoyl indolizine carboxylates by cyclic voltammetry (CV) and differential pulse voltammetry (DPV). It is pursued the influence of concentration on CV and DPV curves and that of the scanning domain and rate on the CV curves. The CV and DPV results are in good agreement. There are established the number and characteristics of the redox processes for each compound. The common features and differences between their electrochemical behaviour were analyzed.

Keywords: methyl-3-benzoyl indolizine carboxylates, cyclic voltammetry, differential pulse voltammetry.

1. Introduction

In recent years, the synthesis of macrocyclic compounds, which can reversibly respond to external (thermal, photochemical, electrochemical, pH, etc.) actions by changing important properties and characteristics (the cavity size, the surface shape, the electronic structure, the complexing ability, etc.) due to the specially introduced functional groups or fragments, has taken a special place in supramolecular chemistry [1]. Such "sensitive" heterocyclophanes containing redox-active biindolizine systems can serve as molecular switches [2] and membrane carriers [3] and are of great interest in the design of new sensors for modern technologies based on molecular processes. Unlike redox-active compounds (ferrocenes, [4-5] tetrathiafulvalenes, [6-7] and quaternized 4,4'-bipyridines [8-9]), biindolizines have found little use as active regions, which make cyclophanes able to respond to external actions, in spite of the fact that biindolizines are quite stable two step redox systems, whose electrochemical behaviour has been studied in sufficient detail [10-15]. Indolizines are π -rich compounds, which are readily oxidized (~ 0.2 - 0.3 V relative to $\text{Fc}^{0/+}$) to form cation radicals [10-14]. The stability and subsequent transformations of

cation radicals are determined primarily by the presence of hydrogen atoms in the pyrrole ring of the indolizine system. The cation radicals and dications of 3,3'-biindolizines, in which all hydrogen atoms in the five-membered ring are replaced by alkyl or aryl groups, are quite stable and can be isolated and characterized as perchlorates [12]. The electrochemical behaviour of two diastereomers of macrocyclic biindolizines, in which both heterofragments are linked at positions 3,3' and, through a bridge, at positions 1,1', is different [13]. Thus, the diastereomer having the anti configuration is oxidized to form stable cation radicals and dications, whereas the oxidation of the diastereomer having the syn configuration is followed by the intramolecular cyclization with the involvement of the C(5) and C(5') atoms of the pyridine rings of the indolizine system having a favourable spatial arrangement [16].

Indolizine derivatives possess valuable biological activity and have been studied for their psychotropic, anti-inflammatory, analgesic, antimicrobial, antiexudative and hypoglycemic effects [17-20]. Certain 1-indolizinols are easily oxidized to stable free radicals [21]. Therefore, Oxygen-protected indolizinols may act as stable precursors for highly potent antioxidants, and it was

found high inhibitory activity against lipid peroxidation in vitro for esters, ethers, carbonates, carbamates and sulfonates of indolizines as well as azaindolizines [22]. In order to establish the mechanism through which these antioxidant properties act, the electrochemical behaviour of several indolizine derivatives, esters, ethers, tosylates, sulfonates and azaindolizines has been investigated by cyclic voltammetry and preparative electrolysis. The CV data obtained were sensitive to the identities of the substituents and were used to characterise the principal oxidation process that took place in each case [20]. There are also some patents that stress the therapeutical effect of certain indolizine derivatives (1-glyoxylamide indolizines) in treating lung and ovarian cancer [23].

The present paper is focused on the electrochemical behaviour of methyl-3-benzoyl indolizine carboxylates: methyl 3-benzoyl indolizine-1-carboxylate (**I1**) and dimethyl 3-benzoyl indolizine-1,2-dicarboxylate (**I2**) (Fig. 1).

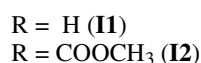
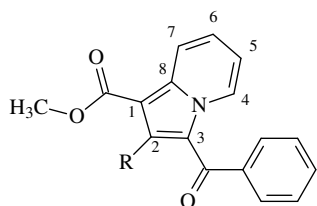


Fig. 1. Structural formula of the investigated indolizines

2. Experimental

Acetonitrile (CH₃CN) and tetrabutylammonium tetraborofluorate (TBABF₄) from Fluka were used as received like solvent and supporting electrolyte. The investigated compounds have been obtained by general procedure for synthesis of indolizines based on 1,3-dipolar cycloaddition reactions of heterocyclic-N-ylides with electron-deficient alkynes or alkenes, according to literature data [24-25].

The experiments were carried out by cyclic voltammetry (CV) and differential pulse voltammetry (DPV) using a PGSTAT12 AUTOLAB potentiostat in a three-compartment cell. The

working electrode was of glassy carbon (diameter of 3 mm), which was polished before each determination with diamond paste (200 μm). The Ag/10 mM AgNO₃ in CH₃CN and 0.1 M TBABF₄ was used as reference electrode. The potential was referred to the potential of the ferrocene/ferricinium couple (Fc/Fc⁺) which in our experimental conditions was 0.07 V. As counterelectrode a platinum wire was used. The determinations were performed at 25 °C under argon atmosphere.

The CV curves were generally recorded at 0.1 V/s or at various rates (0.1-1 V/s) when studying the influence of the scan rate.

3. Results and Discussions

CV and DPV curves were recorded for three concentrations (1-3 mM) of indolizines **I1** and **I2** at different scan rates and domains.

Study of **I1**

The CV and DPV curves for increasing concentrations of the indolizine **I1** are represented in Fig. 2. Only one anodic process is obvious (1a). 3 cathodic processes (1c - 3c) are seen, which are correlated by using the same scale for potentials of both CV and DPV curves.

The influence of the concentration on the DPV peak currents and potentials is shown in Fig. 3 and 4. Linear dependences were found for the peak currents with positive (for anodic processes) or negative (for cathodic processes) slopes. Table 1 and 2 show the equations of these dependences for the influence of concentration on the peak currents and potentials, respectively. 1a shows a positive slope (10 μA/mM), while 1c, 2c and 3c show negative slopes (of about -15; -5; -10 μA/mM). In DPV, the peak potentials are slightly dependent on substrate concentration (slopes of about 10 mV/decade).

From Fig. 2 has been evaluated the influence of concentration on the CV curves. Linear dependences of the CV peak currents and potentials on concentration were found (Fig. 5, Table 3, and Fig. 6, Table 4, respectively). The obtained values show that there is no dependence on concentration for CV peak potentials.

The processes 1a and 1c, corresponding to the formation of the anion radical and cation radical,

respectively, having close values of the peak currents (in absolute value).

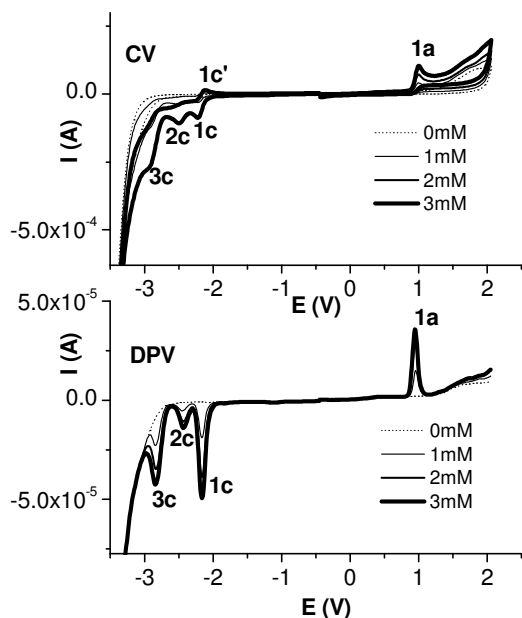


Fig. 2. CV (0.1 V/s) and DPV curves for various concentrations of **II** on glassy carbon electrode ($\Phi = 3$ mm) in 0.1 M TBABF₄, CH₃CN

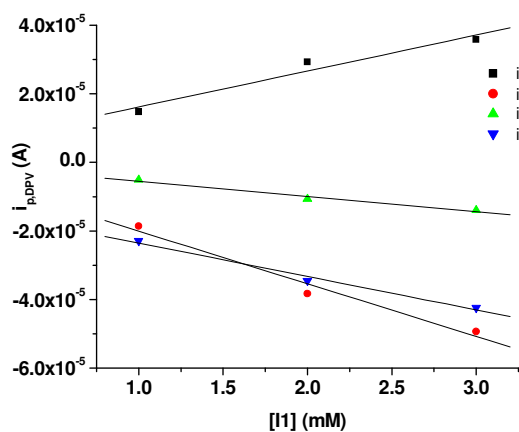


Fig. 3. DPV peak currents dependence on concentration for **II** (same conditions as in Fig. 2)

Table 1. Linear DPV peak currents dependence on concentration for **II**

Peak (DPV)	Y (i, A); X ([I1], mM)
ip,1a	$Y = 5.633E-6 + 1.050E-5 X$
ip,1c	$Y = -4.700E-6 - 1.535E-5 X$
ip,2c	$Y = -1.087E-6 - 4.430E-6 X$
ip,3c	$Y = -1.377E-5 - 9.750E-6 X$

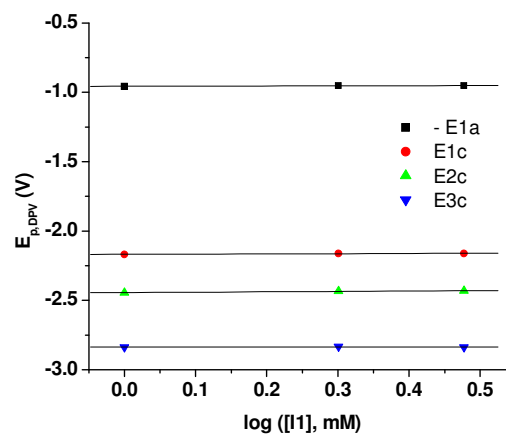


Fig. 4. DPV peak potentials dependence on concentration for **II** (same conditions as in Fig. 2)

Table 2. Linear equations representing the DPV peak potentials dependence on concentration for **II**

Peak (DPV)	Y (E _p , V); X (log [I1], mM)
Ep,1a	$Y = 0.956 - 0.012 X$
Ep,1c	$Y = -2.168 + 0.016 X$
Ep,2c	$Y = -2.443 + 0.028 X$
Ep,3c	$Y = -2.836 + 0.002 X$

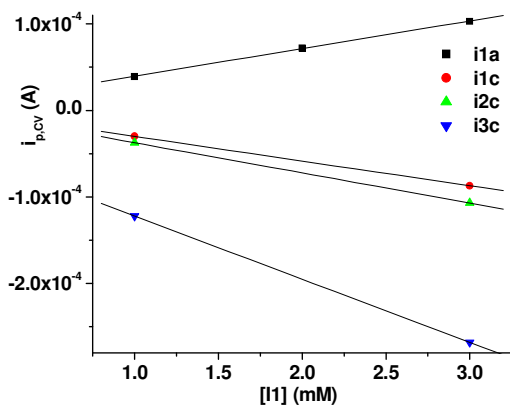


Fig. 5. CV peak currents dependence on concentration for **II**

Table 3. Linear equations representing the CV peak currents dependence on concentration for **II**.

Peak (CV)	Y (i, A); X ([II], mM)
ip,1a	Y = 7.833E-6 + 3.185E-5 X
ip,1c	Y = -1.35E-6 - 2.855E-5 X
ip,2c	Y = -2.45E-6 - 3.485E-5 X
ip,3c	Y = -4.9E-5 - 7.3E-5 X

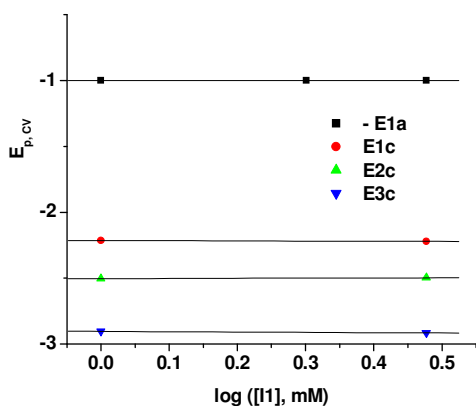


Fig. 6. CV peak potentials dependence on concentration for **II**

Table 4. Linear equations representing the CV peak potentials dependence on concentration for **II**

Peak (CV)	Y (E_p, V); X ($\log [II], \text{mM}$)
Ep,1a	Y = 0.999 - 9.351E-9 X
Ep,1c	Y = -2.215 - 0.012 X
Ep,2c	Y = -2.503 + 0.012 X
Ep,3c	Y = -2.904 - 0.023 X

The influences of the scan rate and range on the CV curves are represented in Fig. 7 and 8.

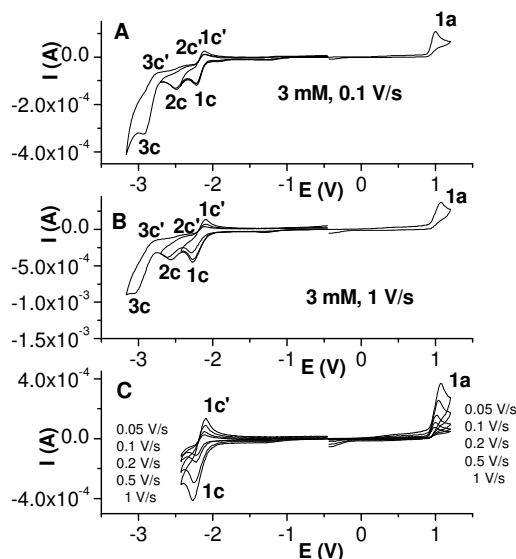


Fig. 7. CV curves for various scan rates and scan domains for **II** (3 mM) on glassy carbon electrode ($\Phi = 3 \text{ mm}$) in 0.1 M TBABF₄, CH₃CN

It can be seen that 1a is an irreversible process while 1c is a reversible one. When scanning till 1c potential (Fig. 7c), in the reverse scan, a counterpeak 1c' can be seen. 2c and 3c are quasi-reversible processes (they have small counterpeaks in the reverse scan 2c', 3c' which can be seen in Fig. 7a and 7b and 8a and 8b).

The influence of the scan rate (between 0.05 and 1 V/s) on the peak currents shows linear dependences on the square root of the scan rate (Fig. 9) with positive slope for 1a and negative slopes for 1c - 3c, while the counterpeak 1c' has also a positive slope (Table 5). As expected, the slopes for 1a and 1c have opposite values (of about $400 \mu\text{A}/\text{V}^{-1/2}\text{s}^{1/2}$).

The peak 3c slope is twice the value of that for 1c and 2c. The peak potentials depend on the scan rate (Fig. 10) with negative slopes for cathodic peaks and positive slopes for anodic peaks (Table 6).

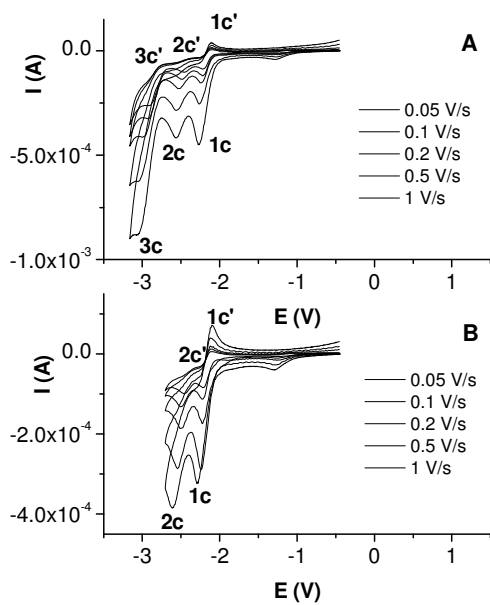


Fig. 8. CV curves for various scan rates and cathodic domains for **II** (3 mM) on glassy carbon electrode ($\Phi = 3$ mm) in 0.1 M TBABF₄, CH₃CN

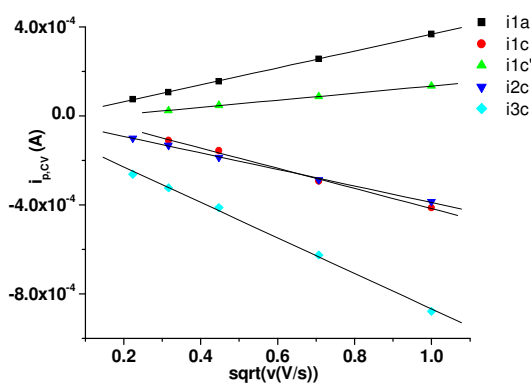


Fig. 9. CV peak currents dependence on scan rate for **II** (same conditions as in Fig. 7 and 8)

Table 5. Linear equations representing the dependence of the CV peak currents (measured in respect to the zero line) on scan rate for **II**

Peak (CV)	Y (i, A); X ($v^{1/2}$, (V/s) ^{1/2})
1a	$Y = -1.170E-5 + 3.793E-4 X$
1c	$Y = 3.729E-5 - 4.538E-4 X$
1c'	$Y = -2.551E-5 + 1.599E-4 X$
2c	$Y = -1.742E-5 - 3.719E-4 X$
3c	$Y = -7.002E-5 - 7.980E-4 X$

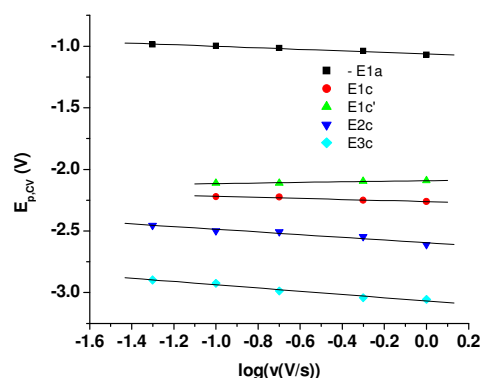


Fig. 10. CV peak potentials dependence on scan rate for **II** (same conditions as in Figs. 7 and 8)

Table 6. Linear equations representing the CV peak potentials dependence on scan rate for **II**

Peak (CV)	Y (E, V); X (log (v, V/s))
1a	$Y = 1.063 + 0.062 X$
1c	$Y = -2.262 - 0.043 X$
1c'	$Y = -2.091 + 0.024 X$
2c	$Y = -2.595 - 0.109 X$
3c	$Y = -3.068 - 0.131 X$

Successive scanning in the domain of the first oxidation process in 3 mM **II** solution in 0.1 M TBABF₄, CH₃CN shows very small differences between cycles (Fig. 11). There is no evident appearance of a film on the electrode surface. The transfer of the modified electrode (after 30 cycles) in 0.5 mM ferrocene in pure electrolyte (0.1 M TBABF₄, CH₃CN) showed no modification of the ferrocene couple on the modified electrode. It seems

that no polymerization occurs on the electrode surface.

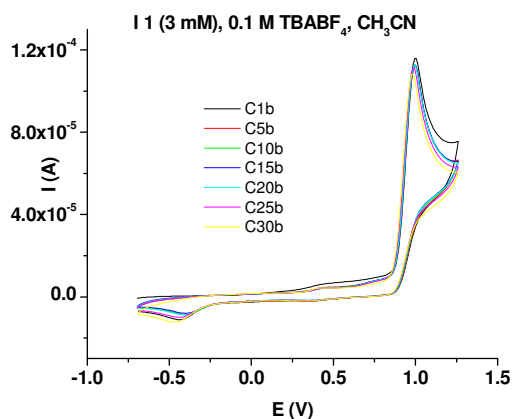


Fig. 11. Successive scans (C1-C30) on glassy carbon electrode ($\Phi = 3$ mm) in order to get films by potential scanning in **I1** solutions (3 mM) in 0.1 M TBABF₄, CH₃CN.

Study of **I2**

Fig. 12 shows the CV and DPV curves obtained for **I2**. Two anodic (1a, 2a) and four cathodic processes (1c - 4c) are observed, which are correlated using the corresponding CV and DPV curves.

The influence of the concentration on the DPV peak currents and potentials is shown in Fig. 13 and 14. Linear dependences were found for the peak currents with positive (for anodic processes) or negative (for cathodic processes) slopes. Table 7 shows the equations of the peak currents versus concentration. The processes 1a and 1c are corresponding to the formation of the anion radical and cation radical. Taking into account the dependence on concentration, the peaks could be separated in two groups, the first one has slopes of the order of 10 μ A/mM (1a, 1c, 3c, 4c) and the second one (2a, 2c) has smaller slopes (2-4 μ A/mM). This could show that 2a and 2c are successive oxidation/reduction processes (to 1a/1c), while 1a, 1c, 3c and 4c are independent processes.

In Fig. 14 and Table 8 are presented the results concerning the influence of concentration on the peak potentials in DPV. Only 2c, 3c and 4c show negative increasing slopes with concentration.

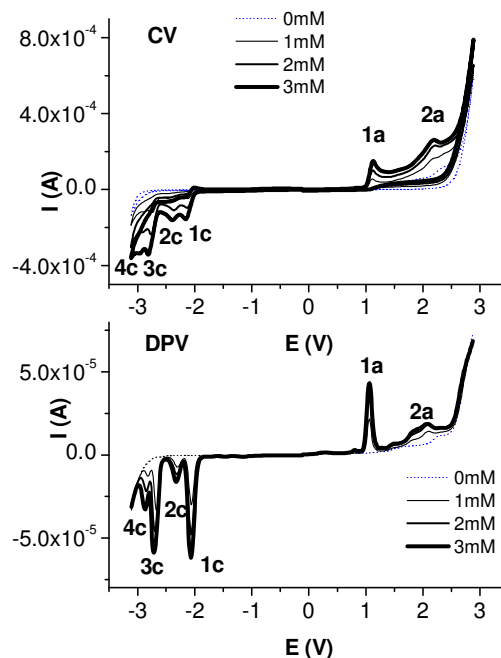


Fig. 12. CV (0.1 V/s) and DPV curves for various concentrations of **I2** on glassy carbon electrode ($\Phi = 3$ mm) in 0.1 M TBABF₄, CH₃CN

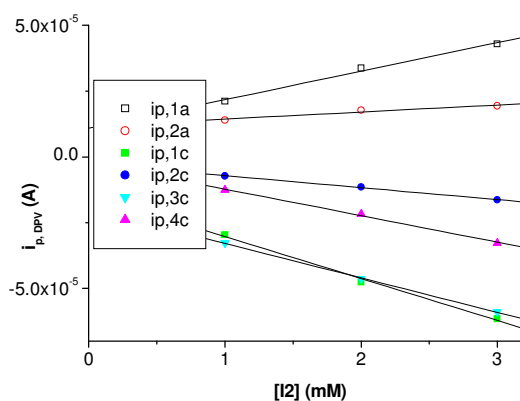
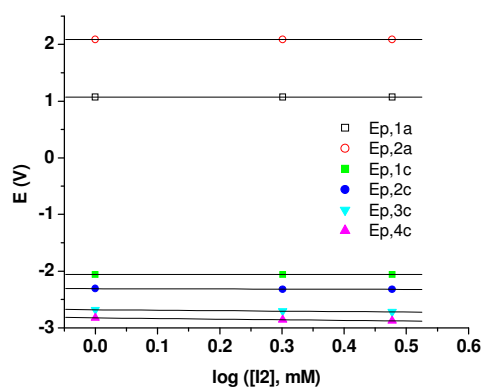


Fig. 13. DPV peak currents dependence on concentration for **I2**

Table 7. Linear equations representing the DPV peak currents dependence on concentration for **I2**

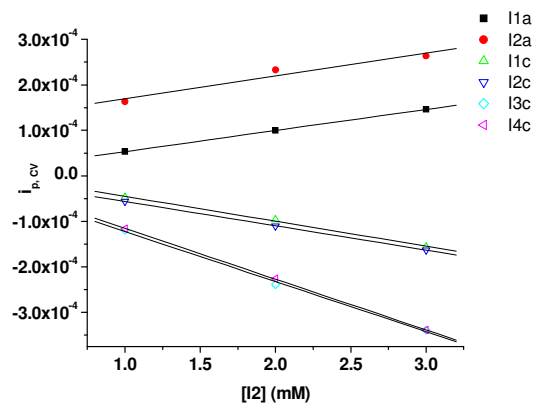
Peak (DPV)	Y (i, A); X ([I2], mM)
ip,1a	Y = 1.090E-5 + 10.84E-6 X
ip,2a	Y = 1.169E-5 + 2.670E-6 X
ip,1c	Y = -1.436E-5 - 15.95E-6 X
ip,2c	Y = -2.616E-6 - 4.550E-6 X
ip,3c	Y = -1.983E-5 - 13.09E-6 X
ip,4c	Y = -2.198E-6 - 1.008E-5 X

**Fig. 14.** DPV peak potentials dependence on concentration for **I2**

The peak currents in CV (Fig. 15 and Table 9) vary linearly with concentration having slopes of about 50 $\mu\text{A}/\text{mM}$ (in absolute value) for 1a, 2a, 1c, 2c, and 100 $\mu\text{A}/\text{mM}$ (in absolute value) for 3c and 4c. These differences could be attributed to the fact that total currents have been considered, as the slopes were found similar in DPV.

Table 8. Linear equations representing the DPV peak potentials dependence on concentration for **I2**

Peak (DPV)	Y (E_p , V); X (log [I2], mM)
Ep,1a	Y = 1.068 + 0 X
Ep,2a	Y = 2.087 + 0 X
Ep,1c	Y = -2.062 + 0 X
Ep,2c	Y = -2.309 - 0.028 X
Ep,3c	Y = -2.681 - 0.080 X
Ep,4c	Y = -2.824 - 0.111 X

**Fig. 15.** CV peak currents dependence on concentration for **I2****Table 9.** Linear equations representing the CV peak currents dependence on concentration for **I2**

Peak (CV)	Y (i, A); X ([I2], mM)
ip,1a	Y = 6.967E-6 + 4.635E-5 X
ip,2a	Y = 1.197E-4 + 5E-5 X
ip,1c	Y = 9.8E-6 - 5.47E-5 X
ip,2c	Y = -3.2E-6 - 5.33E-5 X
ip,3c	Y = -1.233E-5 - 1.1E-4 X
ip,4c	Y = -4E-6 - 1.115E-4 X

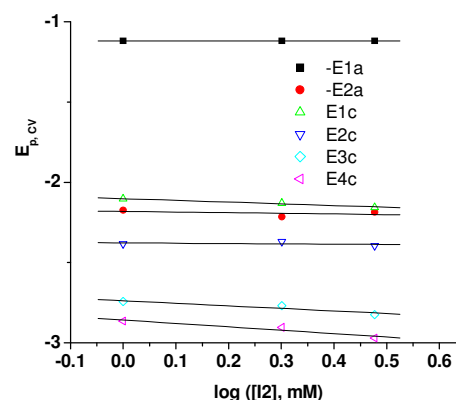
**Fig. 16.** CV peak potentials dependence on concentration for **I2**

Table 10. Linear equations representing the CV peak potentials dependence on concentration for **I2**

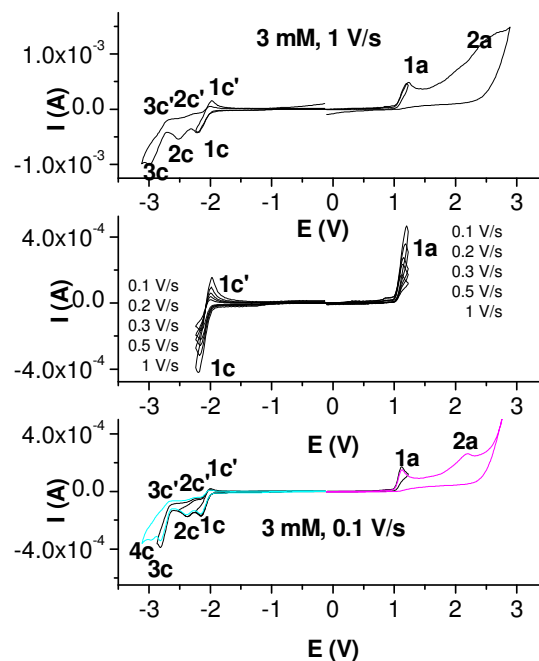
Peak (CV)	Y (E_p, V); X ($\log [I2], mM$)
Ep,1a	$Y = 1.118 + 0 X$
Ep,2a	$Y = 2.181 + 0.039 X$
Ep,1c	$Y = -2.102 - 0.107 X$
Ep,2c	$Y = -2.377 - 0.020 X$
Ep,3c	$Y = -2.738 - 0.159 X$
Ep,4c	$Y = -2.858 - 0.213 X$

The influence of concentration on the CV peak potentials is expressed in Fig. 16 and Table 10. Positive slopes for anodic potentials and negative slopes for the cathodic ones were found.

The influences of the scan rate and scan domain on the CV curves are represented in Fig. 17. It can be seen that 1a and 2a are irreversible processes while 1c is a reversible process. When scanning till 1c potential, in the reverse scan it can be seen a counterpeak 1c'. 2c and 3c are quasi-reversible processes (they have small counterpeaks 2c', 3c' in Fig. 17 in the reverse scan), while 4c is an irreversible process.

1c and 1c' are peaks for a reversible couple **I2/I2⁻** corresponding to the formation of the anion radical. 1a corresponds to the formation of the cation radical from **I2**. The curves show that the formation of the anion radical is a reversible process while the formation of the cation radical is an irreversible process. The oxidation occurs most probably to the N atom of **I2** and is followed by splitting the molecule in small fragments. The reduction occurs to the carbonyl groups. The processes 1c and 2c could be attributed to the reduction of CO groups from the CO-C₆H₅ fragment, and 3c, 4c from COOCH₃ group.

The influence of scan rate on the CV peak currents for 1a, 1c, 1c', 2c, 3c is shown in Fig. 18 and it was found a linear positive dependence for 1a and 1c' and a negative dependence for 1c, 2c, 3c (Table 11).

**Fig. 17.** CV curves for various scan rates and scan domains for **I2** (3 mM)

The influence of scan rate on the CV peak potentials is shown in Fig. 19 and Table 12, which show that the slope for 1a is double in comparison with the slope for 1c, which is almost equal with the slope for 1c'. The values in Table 12 are in agreement with the irreversible character of 1a and the reversible character of the cathodic processes.

A successive scanning in the domain of the first oxidation process in 3 mM **I2** solution in 0.1 M TBABF₄, CH₃CN show very small differences between cycles. The transfer in pure electrolyte shows no evident appearance of a film on the electrode surface.

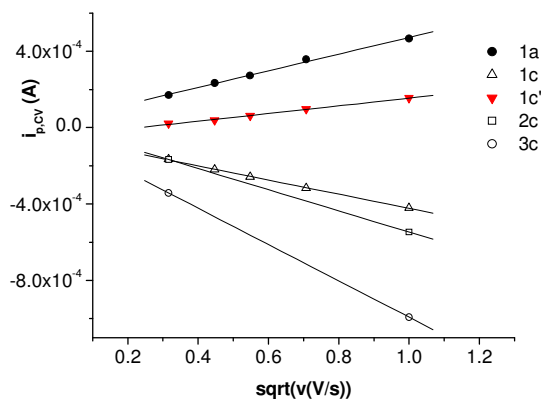


Fig. 18. CV peak currents dependence on scan rate for **I2**

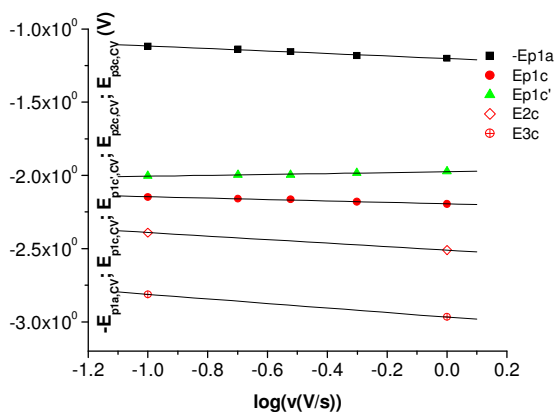


Fig. 19. CV peak potentials dependence on scan rate for **I2**

Table 11. Linear equations representing the CV peak currents (measured in respect to the zero line) dependence on scan rate for **I2**

Peak (CV)	Y (i, A); X ($v^{1/2}$, (V/s) ^{1/2})
1a	Y = 3.623E-5 + 4.361E-4 X
1c	Y = -5.207E-5 - 3.704E-4 X
1c'	Y = -4.677E-5 + 2.011E-4 X
2c	Y = 8.156E-6 - 5.552E-4 X
3c	Y = -4.170E-5 - 9.509E-4 X

Table 12. Linear equations representing the CV peak potentials dependence on scan rate for **I2**

Peak (CV)	Y (E, V); X (log (v, V/s))
1a	Y = 1.202 + 0.086 X
1c	Y = -2.194 - 0.048 X
1c'	Y = -1.975 + 0.031 X
2c	Y = -2.510 - 0.120 X
3c	Y = -2.967 - 0.155 X

Comparison between **I2** and **I1**

By analyzing the results obtained for the two compounds, shown in Fig. 20, it can be observed that they both present an anodic irreversible process (1a) and cathodic reversible (1c) and quasireversible (2c, 3c) processes. **I2** shows a supplementary cathodic process, 4c, probably due to the reduction of the extra -COOCH₃ group.

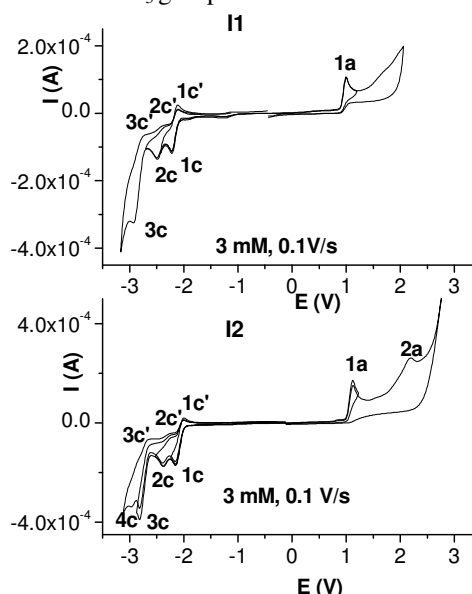


Fig. 20. Comparison between the CV curves of **I1** and **I2** on different scan domains

The degree of reversibility of the first cathodic process (1c) in the two compounds could be evidenced by comparing the difference between the anodic (1c') and cathodic (1c) peak potentials (ΔE_{1c}) with that for the reversible couple Fc/Fc⁺. Table 13 shows that ΔE_{1c} values are quite close to the difference between the peak potentials for the Fc/Fc⁺ couple which was 0.1 V in similar conditions

(the values are higher than those expected because of the uncompensated ohmic resistance of the solution).

From Tables 13 and 14 one can estimate the oxidant and reducing characteristics of the compounds by comparing the potentials of the first anodic (E1a) and cathodic (E1c) peaks. **I1** is easier to oxidize and harder to reduce than **I2**, as shown in Tables 13 and 14. This is in good agreement with the increase of the electron withdrawing effects of two acetate groups with respect to one. The electrochemical stability of **I1** and **I2** was estimated from the difference between the peak potentials for the formation of the cation radical and anion radical (ΔE_{1ac}). It was found that ΔE_{1ac} is bigger for **I2** showing that **I2** is slightly more stable than **I1**, probably due to a more extended conjugation. The CV and DPV data are in good agreement (Tables 13 and 14).

Table 13. Electrochemical CV data of the 1a, 1c, 1c' peak potentials for the two indolizines

Compound	I1	I2
E1a (V)	0.988	1.119
E1c (V)	-2.222	-2.148
E1c' (V)	-2.113	-2.003
ΔE_{1c}^* (V)	0.110	0.145
ΔE_{1ac}^{**} (V)	3.210	3.267

* $\Delta E_{1c} = E_{1c'} - E_{1c}$

** $\Delta E_{1ac} = E_{1a} - E_{1c}$

Table 14. Electrochemical DPV data of the 1a and 1c peak potentials for the two indolizines

Compound	I1	I2
E1a (V)	0.951	1.068
E1c (V)	-2.161	-2.062
ΔE_{1ac}^* (V)	3.113	3.130

* $\Delta E_{1ac} = E_{1a} - E_{1c}$

4. Conclusions

The two investigated methyl-3-benzoyl indolizine carboxylates show similar electrochemical reactivity. The oxidations are irreversible, while the reductions are reversible. The differences in the electrochemical behaviour are in agreement with structural differences.

5. Acknowledgments

MEC (Contract CNMP 71-067/2007)

6. References

- *E-mail address: em_ungureanu2000@yahoo.com
- [1]. J._M. Lehn, *Supramolecular Chemistry, Concepts and Perspectives*, VCH, Weinheim, 1995, 271 pp.
 - [2]. P. D. Beer, *Chem. Soc. Rev.*, 1989, **18**, 409; P. D. Beer, *Adv. Inorg. Chem.*, 1992, **79**.
 - [3]. R. A. Bissel, E. Cordova, A. E. Kaifer, J. F. Stoddart, *Nature*, 1994, **369**, 133.
 - [4]. T. Saji and I. Kinoshita, *J. Chem. Soc., Chem. Commun.*, 1986, 716.
 - [5]. A. M. Allgeier, C. S. Slone, C. A. Mirkin, L. M. Liable-Sands, G. P. A. Yap, and A. L. Rheingold, *J. Am. Chem. Soc.*, 1997, **119**, 550.
 - [6]. Z.-T. Li, P. C. Stein, J. Becher, D. Jensen, P. Mork, and N. Svenstrup, *Chem. Eur. J.*, 1996, 624.
 - [7]. W. Devonport, M. A. Blower, M. R. Bryce, and L. M. Goldenberg, *J. Org. Chem.*, 1997, **62**, 885.
 - [8]. E. Cordova, R. A. Bissel, and A. E. Kaifer, *J. Org. Chem.*, 1995, **60**, 1033.
 - [9]. M. Asakawa, P. R. Ashton, S. E. Boyd, C. L. Brown, R. E. Gillard, O. Kocian, F. M. Raymo, J. F. Stoddart, M. S. Tolley, A. J. P. White, and D. J. Williams, *J. Org. Chem.*, 1997, **62**, 26.
 - [10]. S. Hünig, *Liebigs Ann. Chem.*, 1964, **676**, 32.
 - [11]. S. Hünig and F. Linhart, *Liebigs Ann. Chem.*, 1976, 317.
 - [12]. L. Cardellini, P. Carloni, L. Greci, G. Tosi, R. Andruzzi, G. Marrosu, and A. Trazza, *J. Chem. Soc., Perkin Trans. 2*, 1990, 2117.
 - [13]. M. B. Leitner, T. Kreher, H. Sonnenschein, B. Costisella, and J. Springer, *J. Chem. Soc., Perkin Trans. 2*, 1997, 377.
 - [14]. V. V. Yanilkin, V. A. Mamedov, A. V. Toropchina, A. A. Kalinin, N. V. Nastapova, V. I. Morozov, R. P. Shekurov, and O. G. Isaikina, *Elektrokhimiya*, 2006, **42**, 251 [Russ. *J. Electrochem.*, 2006, **42** (Engl. Transl.)].
 - [15]. H. Sonnenschein, T. Kreher, E. Gründemann, R._P. Krüger, A. Kunath, and V. Zabel, *J. Org. Chem.*, 1996, **61**, 710.
 - [16]. V. A. Mamedov, A. A. Kalinin, V. V. Yanilkin, N. V. Nastapova, V. I. Morozov, A.

- A. Balandina, A. T. Gubaidullin, O. G. Isaikina, A. V. Chernova, Sh. K. Latypov, and I. A. Litvinov, Russian Chemical Bulletin, International Edition, Vol. **56**, No. 10, pp. 2060-2073, October 2007.
- [17]. A.R. Katritzky and C.W. Rees in: W. Flitsch, Editor, Comprehensive Heterocyclic Chemistry **4** Pergamon, Oxford (1984), pp. 443-495.
- [18]. J. Gubin, J. Lucchetti, D. Nisato, G. Rosseeles, M. Chinet, P. Polster and P. Chatelain, J. Med. Chem. **35** (1992), pp. 981-988.
- [19]. R.A. Nugent and M. Murphy, J. Org. Chem. **52** (1987), pp. 2206-2208.
- [20]. Solomon Teklu, Lise-Lotte Gundersen, Frode Rise, Mats Tilset, *Electrochemical studies of biologically active indolizines*, Tetrahedron **61** (2005) 4643-4656.
- [21]. (a) Wadsworth, D. H.; Bender, S. L.; Smith, D. L.; Luss, H. R.; Weidner, C. H. J. Org. Chem. 1986, **51**, 4639-4644. (b) Wadsworth, D. H.; Weidner, C. H.; Bender, S. L.; Nuttall, R. H.; Luss, H. R., J. Org. Chem. 1989, **54**, 3652-3660. (c) Weidner, C. H.; Wadsworth, D. H.; Bender, S. L.; Beltman, D. J., J. Org. Chem. 1989, **54**, 3660-3664. (d) Weidner, C. H.; Michaels, F. M.; Beltman, D. J.; Montgomery, C. J.; Wadsworth, D. H.; Briggs, B. T.; Picone, M. L., J. Org. Chem. 1991, **56**, 5594-5598.
- [22]. (a) Nasir, A. I.; Gundersen, L.-L.; Rise, F.; Antonsen, Ø.; Kristensen, T.; Langhelle, B.; Bast, A.; Custers, I.; Haenen, G. R. M. M.; Wikstrom, H. Bioorg. Med. Chem. Lett. 1998, **8**, 1829-1832. (b) Østby, O. B.; Dalhus, B.; Gundersen, L.-L.; Rise, F.; Bast, A.; Haenen, G. R. M. M. Eur. J. Org. Chem. 2000, **9**, 3763-3770. (c) Østby, O. B.; Gundersen, L.-L.; Rise, F.; Antonsen, Ø.; Fosnes, K.; Larsen, V.; Bast, A.; Custers, I.; Haenen, G. R. M. M. Arch. Pharm. Pharm. Med. Chem. 2001, **334**, 21-24.
- [23]. Hao Li, Keizo Koya, Lijun Sun, Mitsunori Ono, *1-Glyoxylamide Indolizines for Treating Lung and Ovarian Cancer*, US Patent no. A61K 31/437 (2006.01).
- [24]. C. A. Hendrick, E. Ritchie, W. C. Taylor, Austr. J. Chem. Soc., **20**, 1967, p. 2467
- [25]. V. Boekelheide, K. Fahrenholtz, J. Amer. Chem. Soc., **83**, 1961, p. 458.